9th Biennial International Conference
& Exposition on Petroleum Geophysics

"HYDERABAD 2012"

P-129

Integrated studies for sub basalt imaging

Amit Kumar*, Gowri Kalyani Akula, K. K. Hari, *Reliance Industries Ltd.*

Summary

Imaging sub-basalt has long challenged the E & P industry. Significant hydrocarbon strikes in formations below basalt however have continued to spur geophysical improvisations aimed at providing appropriate solutions.

This paper deals with an integrated approach using seismic and CSEM data that was adopted for the imaging the basalt and possibly sub- basalt sediments in offshore West Coast of India. Controlled beam prestack depth migration was carried out on data to generate the final output. The paper also briefly discusses some of the basic work carried out that identifies characteristics as well as issues related to the basalt imaging.

Introduction

Conventional seismic acquisition and processing methods targeting imaging intra- and sub-basalt formations in the West Coast of India have always fallen short of providing unambiguous pictures. Chief reasons for this are:

- Strong reflections due to high impedance contrasts at the top (and bottom) of the basalts leading to significant loss of transmitted seismic energy.
- Scattering of energy due to big acoustic impedance contrast at top and bottom of the basalt. Research has shown that basalt layers scatter the higher seismic frequencies (Pujol and Smithson, 1991; Hobbs, 2002).
- Short period multiples from intra basalt boundaries masking genuine target reflections.
- High attenuation of seismic energy in the basaltic sequences due to its complex internal structure generally causing weak sub-basalt signal.
- Long period multiples, such as those generated between the sea bottom and the top of basalt may obscure sub- basalt reflections & energy reflected from basement.
- Low signal to noise ratio due to the above reasons making estimation of velocity for basalt and sub-basalt sections extremely difficult. Velocity semblances pertaining to primaries are not easily identified.

Considering the above, a solution encompassing the techniques that could mitigate the problems was attempted. It includes:

- Longer offset acquisition (12000 m as opposed to the legacy 6000 m). Long offset data can contain some information which is probably not recorded at shorter offsets as due to higher velocities the reflections emerging into basalts are at relatively higher angles compared to the angle of incidence. Sub-basalt events seen at larger offsets can be fairly large amplitudes due to near critical reflection (Fliedner and White, 2003).
- Low frequency acquisition by towing a deeper cable (18 m) Deep towing of receiver cables can extend the seismic bandwidth towards lower frequencies (Ziolkowski et al. 2003).
- CSEM data acquired over the seismic profile to support identification process of base basalt.
- Use of prestack depth migration to produce final image as PSDM is a better imaging tool. The reflection events below basalt layer are non hyperbolic in nature (Sarkar,2006), which is better handled by PSDM.

Reliance Industries Ltd., Ghansoli, Navi Mumbai.
E-Mail:- Amit.B.Kumar@ril.com

Data Analysis

Some of the basic work and observations on the data is mentioned here.

Analysis of an offset well for basalt velocities

An offset well in the same basin but more than 100 km from the line of interest is the only available well. The sonic velocities in the basalt section are displayed in Figure 1(a).

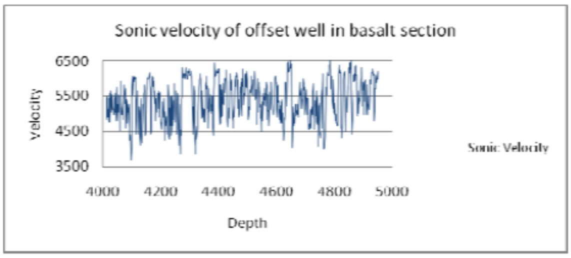

Figure 1(a): Sonic velocity of offset well in basalt showing velocity variations from 3500 to 6500 m/s.

Cross plot of P-wave velocity and S-wave velocity (Figure 1b), and histogram of P wave velocity (Figure 1c) has been displayed.

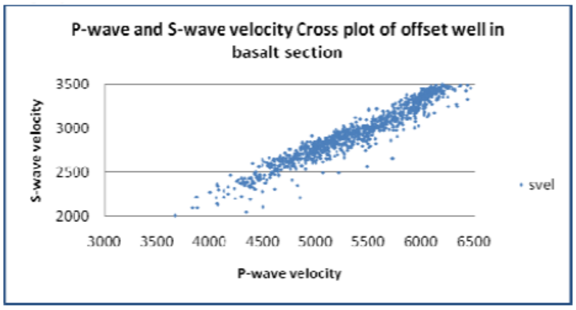

Figure 1(b): P-wave and S-wave cross plot showing velocity variations from 3500 to 6500 m/s.

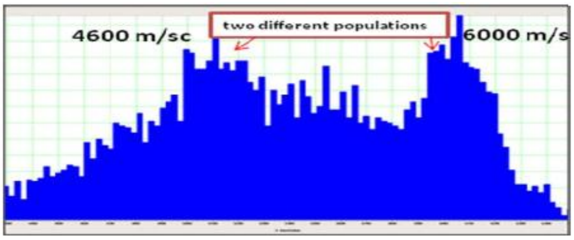

Figure 1(c): Histogram for P wave from the well showing two velocity populations at 4600 m/s and 6000 m/s.

The observations from these are that possible velocity range is from 3500-6500 m/s. The log section shows alterations of thin basalts with variable velocity. Two velocity peaks centering at 4600 m/s and 6000 m/s are seen in the histogram display.

Figure 1(d, e) is a P-wave velocity plot from Atlantic Margin, West of Shetlands (Jeffrey S, 2001) and the basalt velocity indicated as 3500 to 6000 m/s.

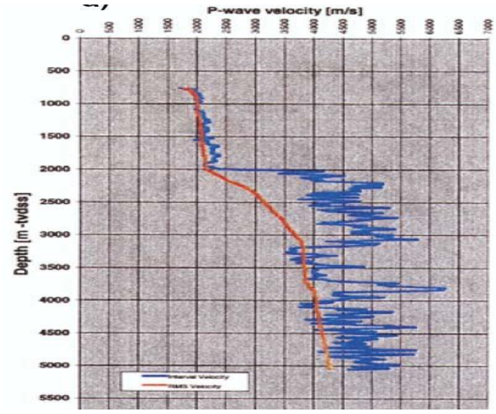

Figure 1(d): Sonic velocity curve at Shetlands.

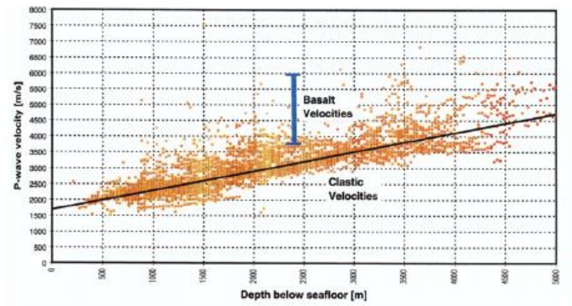

Figure 1(e): Basalt velocity indicating 3500 to 6000 m/s.

Figure 1(f) showing the velocity coherence plots and it is observed that the velocity of volcanic starts from 3700 m/s.

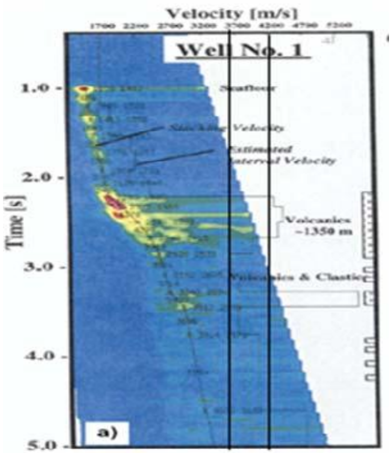

Figure 1(f): Velocity coherence plots.

Velocity from refraction

Considering the raw shot gather (Figure 2) it has been observed that far offset refraction data has useful information. The critical refraction at far offset contains information about the velocity of the layer from where it is refracted as head waves. The wide angle refraction flattens at a LMO velocity of 4600 m/s thus giving an idea about velocity in basalt (Figure 3).

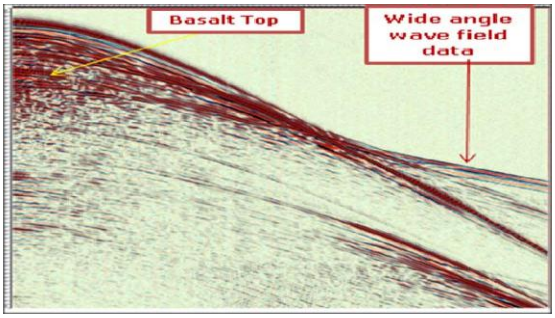

Figure 2: A Shot Gather shows the wide-angle wave- field recorded at long offsets.

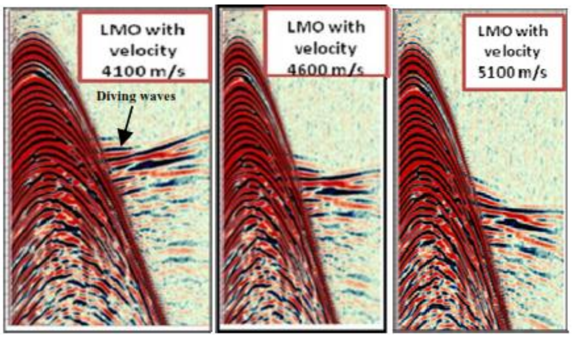

Figure 3: Linear move out at far angle data with different velocities. The perfect LMO velocity is 4600 m/s.

Diving Waves Analysis

In the layer with downward-increasing velocities, diving waves emerging at larger offsets turn deeper within the layer (Figure 3). Eventually the turning rays hit the base of basalt layer and encounter a velocity decrease with depth. At this point the turning rays terminate. No turning rays emerge from the low-velocity sedimentary layer below the basalt. Wide-angle data was obtained by muting the rest of the gather and stacked to image the base of basalt (Figure. 4a, b). (Fliedner and White, 2001)

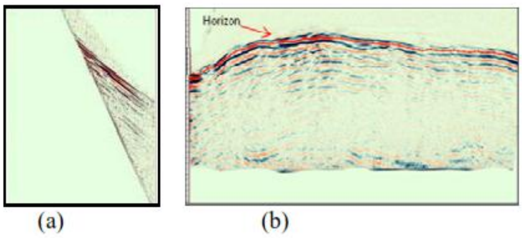

Figure 4: (a) Wide angle gather (b) stack of wide angle gather. (Horizon shows probable base of basalt).

Velocity Scans

Velocity scans indicate presence of lower velocities within probable basalts (In Figure 5,at deeper level the 100% velocity was 2500 m/s but after keeping it 89% of 2500 m/s i.e. 2225 m/s, the events get flatter), indicating likely multiple contamination. Same is visible on semblance panels also. In general the sub basalt signal to noise ratio is very weak, so any strong amplitudes can be attributed to multiple energy (Figure 6).

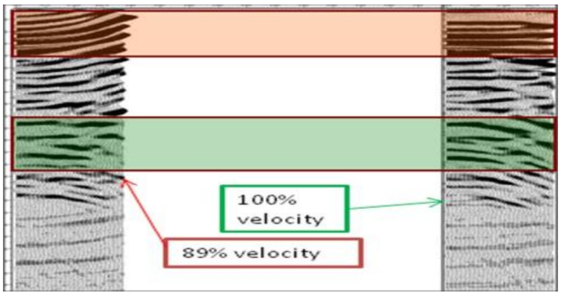

Figure 5: Velocity scan below top of basalt. Scaled down velocity shows the flatter events with respect to initial velocity below top of basalt.

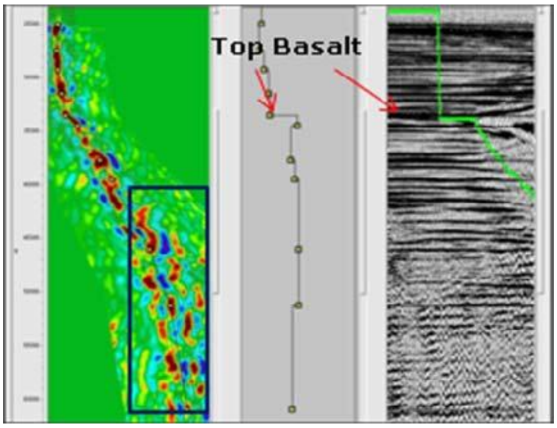

Figure 6: Semblance velocity displays show multiple trends below top of basalt.

Low frequency PSTM

PSTM (Figure. 7a, b) was carried out on legacy data with frequency limited up to 30 Hz i.e. lower side of spectrum and then processed to improve the sub-basalt imaging. (Vishnoi and Sinha, 2010)

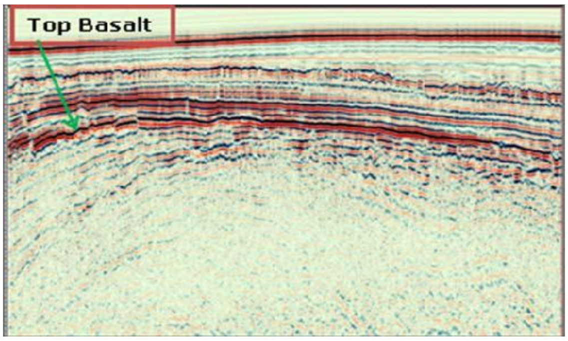

a)

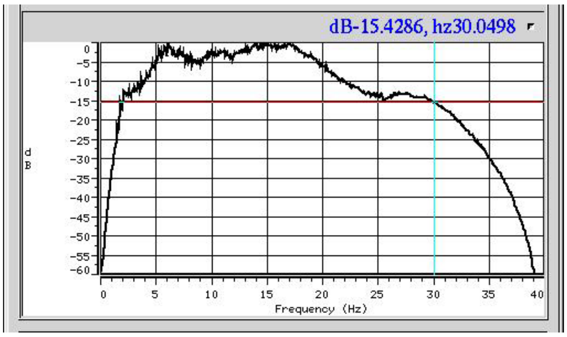

b)

Figure 7: (a) Low frequency data PSTM stack with initial velocity field showing very low signal-to-noise ratio below basalt.
(b) Frequency spectrum having only low frequencies.

Constant offsets stack analysis

In further tests the sensitivity has been checked of full near and far offset of the seismic image. Offset stacks have been prepared for raw dataset to image the basement (Figures 8, 9, 10).

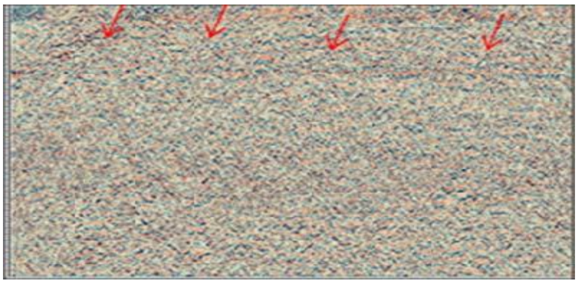

Figure 8: Full offset Stack in the deeper part (below top of basalt). No- major events are observed at deeper level.

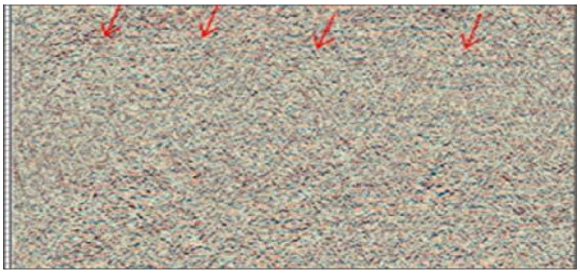

Figure 9: Near offset stack in the deeper part(below top of basalt); still no major events observed at deeper level.

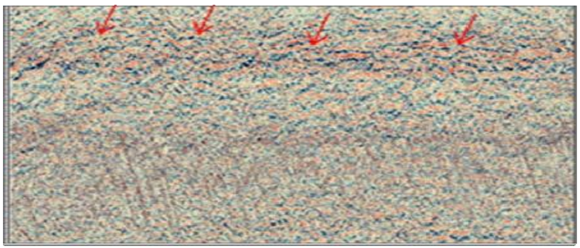

Figure10: Far offset stack in the deeper part(below top of basalt). Some low frequency events are observed which were not in full offset and near offset.

Integrated study

The processing exercise was carried out with the following objectives :

- To image sub basalt rift cycles associated with episodic volcanism and to improve poor ssignal-to-noise ratio within and below basalt.
- To get the correct velocity of basalt.
- To get the basalt layer thickness.

The acquired data was preprocessed before time and depth migration to remove noise and multiples using standard processing steps. The work flow of PSTM and PSDM is been shown in Figure. 11.

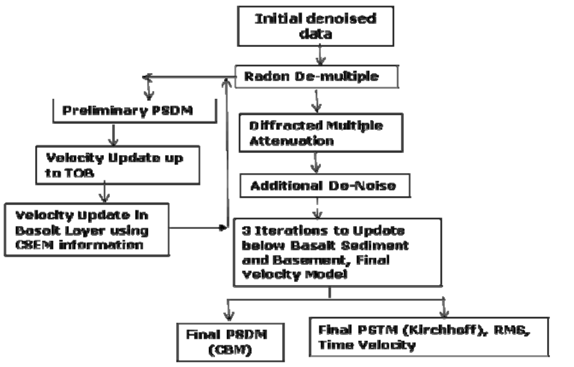

Figure 11: PSDM and PSTM workflow. Note that PSDM has been performed before PSTM for refining the velocity model.

CSEM provided a resistivity section wherein the basalt layer can be identified by its high resistivity. CSEM data set is only used for the rough idea of basalt boundaries to start the initial model in depth domain.

A depth migration was carried out with velocity updated up to the top of the basalt by tomography. The next stage was applying constraints using CSEM data, i.e. CSEM has been taken as guide to mark basalt boundaries (Figure 12).

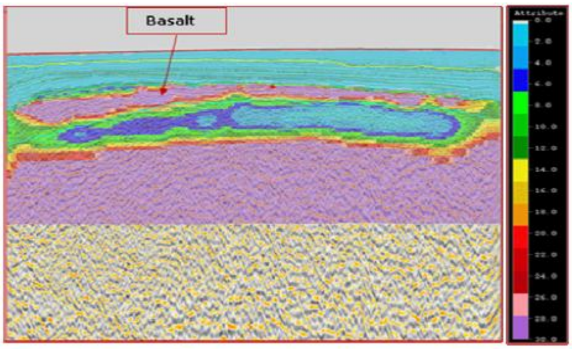

Figure12: CSEM resistivity map overlaid on seismic section. High resistivity purple layer is considered as basalt.

The section below the top of the basalt was subjected to migration scans using a range of velocities to obtain a velocity that ensured a match of the probable base of basalt with the CSEM derived base of basalt. (Figures 13, 14).

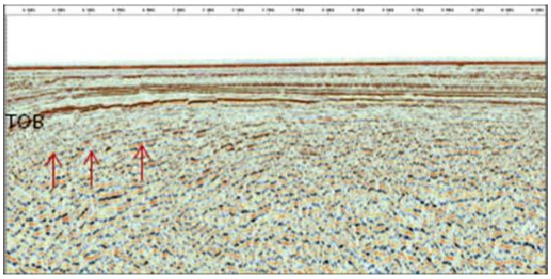

Figure 13: PSDM stack with velocity update up to top of basalt. There is no boundary seen for base of basalt.

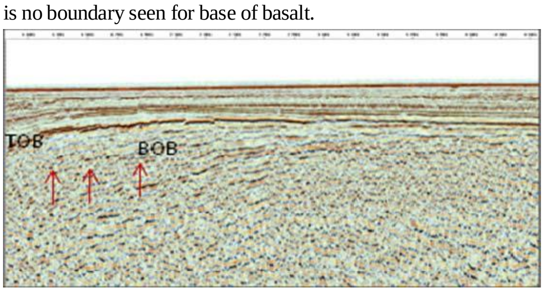

Figure14: PSDM stack obtained by using CSEM dataset for velocity update up to base of basalt. The base of basalt boundary is more prominent now.

After freezing the basalt velocity, migration velocity scans were used to generate the optimum model for sub basalt formations.

Results and Discussions

The final interval velocity model in depth is shown in Figure 15. A controlled beam prestack depth migration was carried out using the final velocity model. Beam migration was preferred over Kirchhoff as it handles noise better and accounts for multi-pathing of the rays. The controlled beam depth migrated gathers and stacks (converted to time) are shown in Figure16 and Figure 17 respectively. The derived basalt interval velocity is around 3700 m/s.

With reference to offset well analysis and the referenced information from Shetlands area, it is inferred here that the seismic velocity observed is in the lower side of mean basalt velocities (4500 to 4600 m/s). It may indicate that the basalt zone is an alteration of low and high velocity volcanic streaks or a mix of volcanic and clastics.

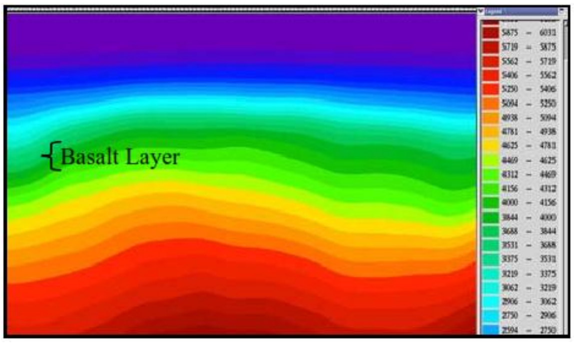

Figure15: Final depth velocity model.

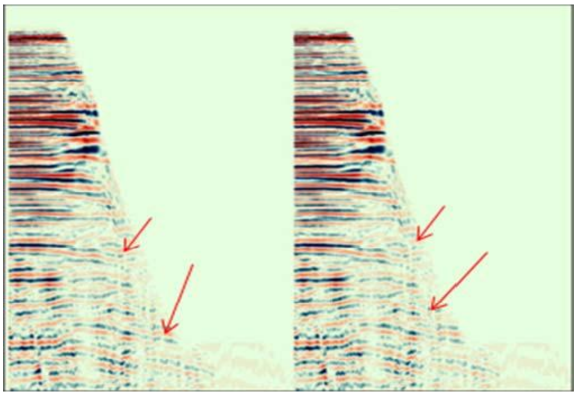

Figure 16: Final PSDM gathers in time. Events at sub-basalt region are more focused and visible than in PSTM gathers in (Figure 19).

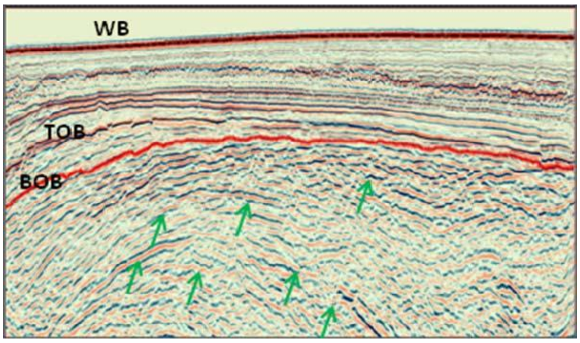

Figure 17: Final PSDM (Beam) stack in time with final velocity model. Probable base of basalt horizon is overlaid on the section. Events at sub-basalt region are more focused and visible than in PSTM stack in (Figure 20).

This interval velocity model was converted to the RMS velocity model in time (Figure 18).

Radon demultiple applied again on the data as we have now much better velocity than the initial stage. After Radon demultiple PSTM has been done on the data. The PSTM gathers and stack are shown in Figure19 and 20 respectively.

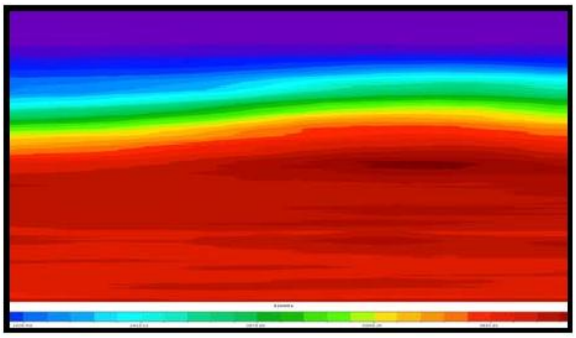
Figure 18: RMS velocity field for PSTM.

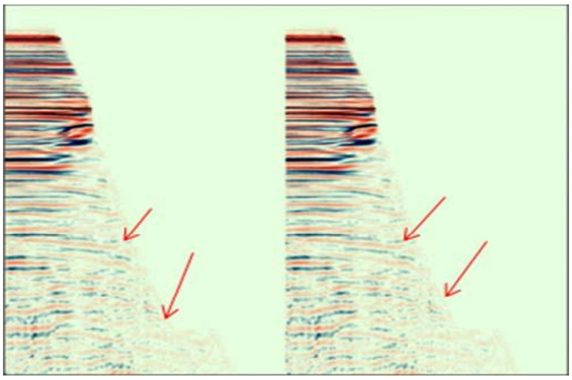
Figure 19: PSTM gathers. The signal-to-noise ratio at sub-basalt region is not as good as in PSDM (controlled beam migration) gathers (Figure 16)

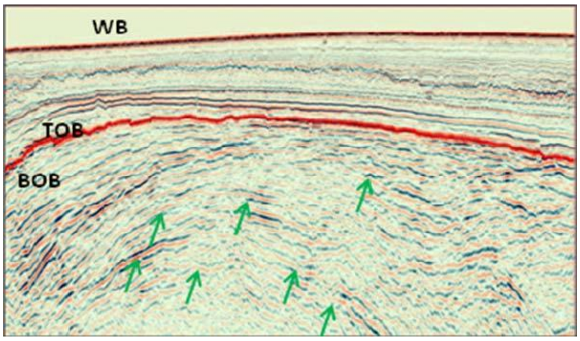

Figure 20: Final PSTM Stack overlaid with top of basalt horizon. The signal to noise ratio at sub-basalt region is not as good as in PSDM (controlled beam migration) stack (Figure 17)

Conclusions

Integration of different geophysical technologies and methodologies are needed for imaging below basalt.

These initial results show that processing of deep towed long offset data in depth domain with the help of CSEM data sets generated a better image with higher amplitude and corelatable events from sub-basalt section compared to time domain. Better defined structures and improved continuity of the horizons in the depth migration over time migration output is also observed.

We also observed that the PSTM (Figure 20) done by the RMS velocity converted from interval velocity of beam migration produced better results than the PSTM done on conventional data (Figure 7a).

Future Work

Since dramatic elastic-impedance contrasts between the high velocity layer and regional sedimentary framework cause P-wave energy to be converted to shear-wave (S-wave) energy so in future course of work we will emphasize on the potential of multicomponent data applications in the basaltic environment.

References

A.K.Sarkar, P.V.Rao, S. Panigrahi and S.R.M.Karnawat, 2006, Enhancing sub-basalt imaging using depth domain processing: 6th Biennial International Conference & Exposition on Petroleum Geophysics.

Fliedner, M., and White, R., 2003, Depth imaging of basalt flows in the Faeroe-Shetland Basin: Geophys.J. Int., 152, 353-371.

Hobbs R. 2002. Sub-basalt imaging using low frequencies. Sub-basalt imaging 9–11th April, 2002 Cambridge, UK. Journal of Conference Abstracts 7, 152–153

Jeffrey S. Ogilive, Texaco International, Houston, Texas, U.S.,Richard Crompton, Paradigm Geophysical, Slough, U.K, Nicholas M. Hardy, Texaco Britain Ltd., London, U.K., Jan 2001, Characterization of volcanic units using detailed velocity analysis in the Atlantic Margin, West of Shetlands, United Kingdom : The Leading Edge , 34–50.

Joseph W. Gallagher and Peter W. Dromgoole, 2008, seeing below the basalt- offshore Faroes: Geophysical Prospecting, 56, 33-35.

Moritz m. Fliedner and Robert S. white, 2001, Seismic structure of basalt flows from surface seismic data, borehole measurements, and synthetic seismogram modeling: Geophysics, 66, 6, 1925–1936.

Pujol J. and Smithson S. 1991. Seismic wave attenuation in volcanic rocks from VSP experiments. Geophysics 56, 1441–1455.

Vishnoi DK and Sinha DP, 2010, Low Frequency Migration Technique to image fractures below sub-basalt or Trap- A Brief Analysis: 8th Biennial International Conference & Exposition on Petroleum Geophysics.

Ziolkowski, A., Hanssen, P., Gatliff, R., Jakubowicz, H., Dobson, A., Hampson, G., Li, X. Y., and Liu, E. R. [2003] Use of low frequencies for sub-basalt imaging. Geophysical Prospecting, 51, 3, 169-182.

Acknowledgement

The authors are thankful to Reliance Industries Ltd. for giving them the necessary permissions to present this research paper in the SPG-2012 conference, at Hyderabad. Authors are also grateful to Mr. A. K. Biswal and Mr. M.K. Balasubramanium of RIL for their continued support and guidance. The authors are grateful to Geo-data Processing facility, RIL, KK asset team, RIL, and CGGV, Mumbai, for their kind technical support for the data sets used in this study.